Proc. Natl. Acad. Sci. USA
Vol. 88, pp. 897–901, February 1991
Neurobiology

In vitro neurons in mammalian cortical layer 4 exhibit intrinsic oscillatory activity in the 10- to 50-Hz frequency range

(persistent sodium conductance/conjunctive properties/cognition)

RODOLFO R. LLINÁS*†, ANTHONY A. GRACE‡, AND YOSEF YAROM§

*Department of Physiology and Biophysics, New York University Medical Center, New York, NY 10016; ‡Department of Behavioral Neuroscience & Psychiatry, University of Pittsburgh, Pittsburgh, PA 15260; and §Department of Neurobiology, Institute of Life Sciences, Hebrew University of Jerusalem, Jerusalem, Israel

Contributed by Rodolfo R. Llinás, October 29, 1990

ABSTRACT **We report here the presence of fast subthreshold oscillatory potentials recorded *in vitro* from neurons within layer 4 of the guinea pig frontal cortex. Two types of oscillatory neurons were recorded: (*i*) One type exhibited subthreshold oscillations whose frequency increased with membrane depolarization and encompassed a range of 10–45 Hz. Action potentials in this type of neuron demonstrated clear after-hyperpolarizations. (*ii*) The second type of neuron was characterized by narrow-frequency oscillations near 35–50 Hz. These oscillations often outlasted the initiating depolarizing stimulus. No calcium component could be identified in their action potential. In both types of cell the subthreshold oscillations were tetrodotoxin-sensitive, indicating that the depolarizing phase of the oscillation was generated by a voltage-dependent sodium conductance. The initial depolarizing phase was followed by a potassium conductance responsible for the falling phase of the oscillatory wave. In both types of cell, the subthreshold oscillation could trigger spikes at the oscillatory frequency, if the membrane was sufficiently depolarized. Combining intracellular recordings with Lucifer yellow staining showed that the narrow-frequency oscillatory activity was produced by a sparsely spinous interneuron located in layer 4 of the cortex. This neuron has extensive local axonal collaterals that ramify in layers 3 and 4 such that they may contribute to the columnar synchronization of activity in the 40- to 50-Hz range. Cortical activity in this frequency range has been proposed as the basis for the "conjunctive properties" of central nervous system networks.**

Neurons in the mammalian central nervous system demonstrate two distinct modes of firing. In one case neuronal firing is firmly determined by excitatory and inhibitory synaptic inputs and subserves basic communication within and among neuronal networks. The other mode is characterized by rhythmic oscillatory neuronal firing and by intrinsically triggered membrane potential oscillations. This latter type of activity is modulated, rather than controlled, by synaptic input and is thought to underlie cyclic events such as the alpha rhythm (1), the hippocampal theta rhythm (2), and physiological tremor (3–5).

Commonly, rhythmic firing patterns in central nervous system neurons have been shown to be mediated by the sequential activation of a set of conductances, of which the most prominent have been calcium-dependent (6). Thus, in a typical model of rhythmic activity, increase in a voltage-gated calcium conductance (which may be regenerative) triggers a transient increase in intracellular calcium concentration, which in turn activates a calcium-dependent potassium conductance [$g_{K(Ca)}$]. The resulting membrane hyperpolarization then leads to a rebound low-threshold calcium conductance that reinitiates the cycle and sustains the oscillatory activity (4).

Exceptions to this mechanism were revealed in studies of membrane oscillations in entorhinal cortical neurons (7), neocortical interneurons (8), and parabrachialis neurons in the rostral brainstem (9). In all of these, subthreshold oscillations depended on an increased conductance to sodium, rather than to calcium. Intrinsic activity in these three cell types related to well-known central nervous system rhythms. Thus, the entorhinal neurons oscillate at 5–7 Hz (near the theta rhythm), the parabrachialis neurons at close to 10 Hz (near the alpha rhythm), and the cortical neurons at frequencies ranging from 10 to 50 Hz (near that reported for the activated cortical rhythm).

The intrinsic electrophysiology of cortical neurons is of particular interest since it was reported (10) that visual stimulation elicits rhythmic firing of visual neurons at 42 ± 7 Hz in a given cortical column in the visual cortex and that these oscillations may be in phase with the oscillation of functionally related cortical columns. This synchronized activity was proposed to provide a functional link between related stimuli that are spatially separated over the visual cortex and was thought to arise within individual cortical columns (10, 11). Since the characterization of this rhythm was based on field potential and extracellular multiunit activity recordings, the cellular mechanisms responsible for such activity have not been explored. *A priori* it would seem plausible that the generation of this rhythmicity would include a neuronal pool capable of intrinsic oscillation near 40 Hz. Such a pool, if properly interconnected, could synchronize activity within the cortical columns.

We report here the electrophysiological properties of interneurons in layer 4 of the frontal cortex of the guinea pig. These cells exhibit high-frequency membrane potential oscillations in which the activation of a sodium-dependent tetrodotoxin (TTX)-sensitive conductance plays a prominent role. The axonal and dendritic fields of a subcategory of these cells, as revealed by intracellular staining, indicate that they may represent a class of inhibitory interneurons.

MATERIAL AND METHODS

By following standard procedures used in our laboratory (12), 300- to 400-μm coronal brain slices were made from the frontal cortex of the adult guinea pig. After a 1-hr incubation in oxygenated Krebs–Ringer solution containing 124 mM NaCl, 5 mM KCl, 1.2 mM KH_2PO_4, 2.6 mM $MgSO_4$, 2.4 mM $CaCl_2$, 26 mM $NaHCO_3$, and 10 mM glucose and equilibrated

The publication costs of this article were defrayed in part by page charge payment. This article must therefore be hereby marked "*advertisement*" in accordance with 18 U.S.C. §1734 solely to indicate this fact.

Abbreviations: TTX, tetrodotoxin; AHP, after-hyperpolarization; IPSP, inhibitory postsynaptic potential.

†To whom reprint requests should be addressed at: Department of Physiology and Biophysics, New York University Medical Center, 550 First Avenue, New York, NY 10016.

with 95% air/5% CO_2, the slices were transferred to a recording chamber and superfused with a similar solution. In some experiments TTX was added to the superfusate (final concentration, 10 μM) to block the voltage-dependent persistent sodium current and the fast sodium-dependent action potentials. The temperature of the chamber was maintained at 37°C, since spontaneous spike activity was rarely observed at lower temperatures.

Intracellular recordings were obtained using micropipettes filled with 3 M potassium acetate and an Axoclamp II amplifier (Axon Instruments, Burlingame, CA) in the conventional bridge-current clamp mode. Intracellular recordings were considered suitable for analysis if they were obtained from neurons having a resting membrane potential of at least −60 mV and an input resistance >20 MΩ. The intracellular potentials were displayed on an oscilloscope and stored on videotape after digitization using a Neurocorder (Neurodata, New York).

Cells were stained by intracellular injection of Lucifer yellow (13) or horseradish peroxidase (14, 15) and processed by standard procedures (16).

RESULTS

General Electrophysiological Properties. Intracellular recordings were made from neurons in all layers of the frontal portion of the neocortex. These cells were categorized according to their action potential waveform and firing pattern. From a data base consisting of several hundred neurons, 57 layer 4 neurons demonstrated intrinsic oscillatory properties. Neurons were divided into two categories—those demonstrating a wide range of subthreshold oscillatory frequencies (10–45 Hz, n = 37) and those demonstrating a narrow-frequency range (35–50 Hz, n = 20).

Broad-frequency oscillators. The broad-range oscillators fell into three categories according to small differences in their spike properties. One was characterized by a relatively wide action potential (>1.2 msec at half amplitude) and a prolonged after-hyperpolarization (AHP) (>100 msec at half amplitude). An example of such a cell is shown in Fig. 1*A*; the two superimposed traces represent the responses to threshold current pulses. The most characteristic feature of this type of cell is the AHP that reached a peak immediately after the spike and had a slow, almost linear, decay.

The second type had relatively narrow action potentials (<0.8 msec at half amplitude) and an AHP that reached its maximum value immediately after the spike and returned to the baseline with two exponential components (Fig. 1*B*). The third type of neuron had intermediate spike characteristics (Fig. 1*C*) (duration at half amplitude near 1 msec) and an AHP that reached its peak amplitude slowly, over a period of 20–40 msec.

The three types of neurons did not differ in their resting potential level (average, 63 mV; n = 37; range, 59–72 mV) or input resistance (30 ± 15 MΩ). As shown in Fig. 1 *D–F*, the current–voltage curves were linear from +5 mV to −15 mV.

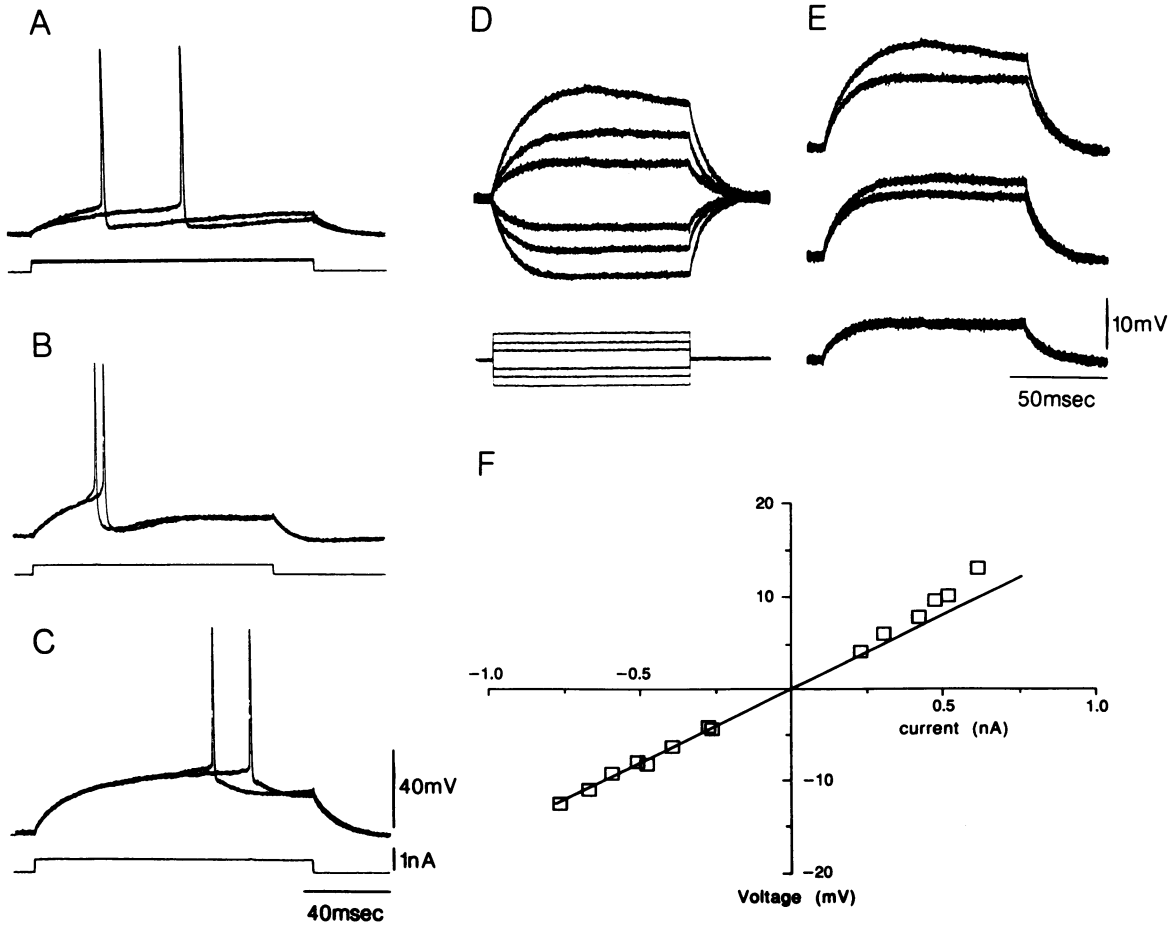

FIG. 1. Intracellular recordings from neurons in layer 4 of the frontal cortex. (*A–C*) Various types of action potentials encountered in broad-frequency oscillating neurons. Note the differences in the AHPs. For further details see text. (*D* and *E*) Input resistance as determined by hyperpolarizing and depolarizing step current pulses. (*E*) Superposition of hyperpolarizing and depolarizing pulses to demonstrate presence of a persistent inward conductance upon membrane depolarization. The effect of this persistent current can also be seen in *F* where the voltage for the more depolarized current injections deviated upward from a linear current–voltage relationship.

At more depolarized levels, however, a clear deviation from linearity was always observed. Since it is likely that this deviation plays an important role in the generation of the subthreshold oscillations, we investigated its properties by comparing pairs of membrane responses elicited by current pulses with identical amplitude and duration but opposite polarity. To facilitate comparison, the hyperpolarizing response was inverted and superimposed on its depolarizing partner. As shown in the two largest responses in Fig. 1*E*, at levels >5 mV, the depolarizing responses were larger than the hyperpolarizing responses. It is clear from this comparison that the deviation from linearity is due to the activation of a voltage-dependent persistent inward current. As demonstrated in previous studies, this slow depolarization is often generated by a voltage-gated persistent sodium current (12, 17, 18).

Narrow-frequency oscillators. The action potentials of cells that oscillate within a narrow-frequency range were easily distinguished from those described above based on the absence of a pronounced AHP. Indeed, as illustrated in Fig. 2*D* (six superimposed spikes), the duration of the AHP was in the order of 26 msec. Their spike duration was close to 1 msec at half amplitude (Fig. 2*E*, six superimposed spikes) with a spike height of 79.4 ± 6 mV (mean ± SEM).

Subthreshold Oscillatory Properties. *Broad-frequency oscillators.* Spontaneous oscillations were present at the resting potential in 18 of the 37 neurons; in the remaining 19 cells membrane-potential oscillations were triggered by membrane depolarization. Injection of a low-amplitude (0.3 nA) current pulse elicited a brief burst of action potentials followed by irregular single-spike firing as shown in the lower trace of Fig. 3*A*. The single action potentials arose from threshold membrane potential oscillations. A larger-amplitude (0.6 nA) current injection (Fig. 3*A*, upper trace) elicited a longer initial spike burst followed by shorter bursts. Recordings from the same cell are displayed at faster sweep speed in Fig. 3*B*. These three sweeps were obtained at the same membrane potential. Note the correspondence between the action potentials and subthreshold oscillations.

The relationship between oscillation frequency and membrane potential is shown in Fig. 3 *C* and *D*. These traces, which illustrate subthreshold oscillations increasing in frequency with membrane depolarization, were obtained from recordings similar to those shown in Fig. 3*A*. The plot in Fig. 3*D* shows the linear relationship between membrane oscillation frequency (measured by autocorrelation) and membrane potential.

The sodium dependence of this oscillatory phenomenon is shown in Fig. 3 *E* and *F* in the same cell as illustrated in Fig. 3*A*. The control record shown in Fig. 3*E* demonstrates the activity obtained in a cortical neuron following a 0.6-nA step depolarization (the amplitude of the action potentials was truncated). As in Fig. 3*A*, the initial burst of activity was followed by regular firing that appeared to be triggered by subthreshold oscillations. The oscillations in this cell were completely blocked 30 sec after addition of TTX (10 μM) to the perfusate (Fig. 3*F*, top trace), whereas blockade of the action potentials required 1.5 min of exposure to the TTX (Fig. 3*F*, lower trace).

Narrow-frequency oscillations. Subthreshold oscillations at nearly constant frequencies could be elicited, or occurred spontaneously, in 20 neurons. Recordings from three such cells are shown in Fig. 2. Single oscillations usually lasted 22–28 msec and had an average amplitude of 5.9 ± 2.1 mV. Spontaneous subthreshold oscillations were rarely observed at the resting membrane potential (beginning of traces in Fig. 2 *A*, *B*, and *F*) but were found upon membrane depolarization. These cells demonstrated a clear non-inactivating sodium-dependent plateau potential. Subthreshold oscillations [that could outlast the current pulse that elicited them (Fig. 2 *A* and *B*)] were generated on the plateau potential. The average frequency at 37°C was 44.7 ± 4.64 Hz (n = 20) as determined from autocorrelograms such as that in the inset in Fig. 2*A*. In this type of cell, a depolarizing pulse (arrows, Fig. 2*C*) delivered during the subthreshold oscillation (elicited

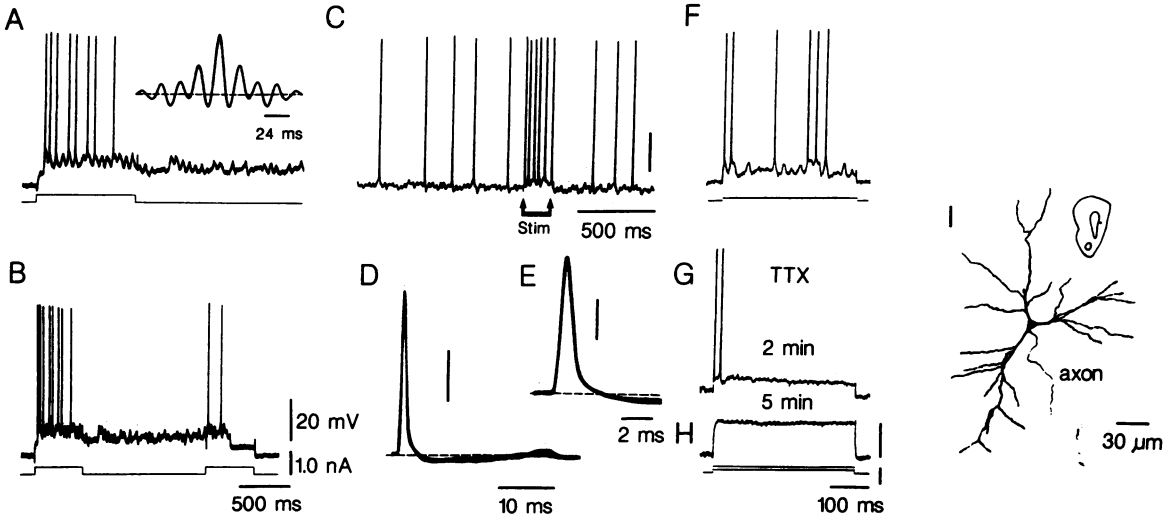

FIG. 2. Electrophysiology of sparsely spinous neurons of the cortex. (*A*) Subthreshold oscillation at approximately 42 Hz generated by a depolarizing current pulse. The autocorrelogram shows a 24-msec peak-to-peak interval. (*B*) Same recording as *A* but at a slower sweep speed demonstrates the all-or-none nature of oscillatory events. The first pulse generated an oscillatory response that outlasted the duration of the stimulus. The second pulse depolarized the cell slightly and produced two action potentials. Note that the subthreshold oscillatory frequency was not modified by the prolonged current pulse (*A* and *B*). The plateau potential that generated the oscillation disappeared abruptly in the middle of the second current pulse. (*C*) Subthreshold oscillation in another neuron having a frequency of the order of 38 Hz and generated by a DC current injection. Upon further depolarization (between arrows) spikes were generated at the peaks of subthreshold oscillatory events without modifying the oscillatory frequency. (*D*) Superposition of six action potentials from the cell in *C* demonstrates their time course and AHP waveform. (*E*) Characteristics of the action potentials are illustrated at a faster sweep speed. (*F–H*) Effect of TTX on a third cell. (*F*) Control. (*G*) TTX blocked the oscillatory potentials after 2 min. (*H*) TTX blocked all activity after 5 min. (Differences in the blocking time between these records and those in Fig. 3*E* reflect a difference in the depth of the recorded cells rather than a different sensitivity to TTX.) (*I*) Camera lucida drawing of narrow-frequency oscillatory neuron labeled intracellularly with horseradish peroxidase. (*Inset*) Location of neuron in cortical layer 4.

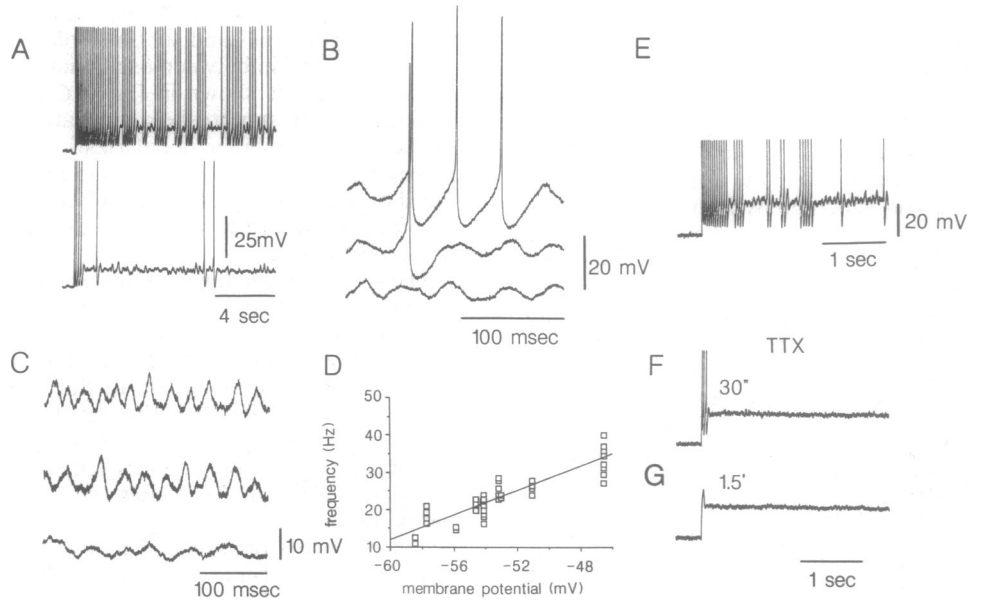

FIG. 3. Properties of broad-band oscillating neurons. (*A*) Firing response of the cells to a prolonged depolarizing current injection (0.6 nA). The action potentials fired at regular frequencies and, in their absence, subthreshold oscillations were observed, especially in a lower trace at a lower depolarization level (0.3 nA). Note the presence of large AHPs with amplitudes in the order of 10–15 mV. (*B*) Illustration of the relationship between membrane potential and spike generation. The lower traces were recorded at 3, 5, and 7 mV (top, middle, and bottom trace, respectively) from the resting potential. (*C*) Examples from another neuron of the relationship between three levels of depolarization similar to those in *B* and subthreshold oscillation. (*D*) Plot of membrane potential versus the frequency of oscillation showing a range of 10–40 Hz. Control oscillation before (*E*) and 30 sec (*F*) and 1.5 min (*G*) after bath administration of TTX.

here by DC depolarization) increased the likelihood that the oscillation would reach spike threshold, the spiking occurring at the peak of the oscillatory potentials. Note, however, that in contrast to cells with a broad frequency of oscillations, DC membrane depolarization did not alter the oscillatory frequency.

The ionic mechanism for the oscillation in these cells was similar to that for the broad-frequency oscillators. The control prior to TTX is shown in Fig. 2*F*. Addition of TTX initially blocked the subthreshold membrane potential oscillations (Fig. 2*G*) and then the spike generation (Fig. 2*H*), very much as observed for the broad frequency oscillation cells (Fig. 3*E*).

Six neurons with narrow-frequency membrane oscillations were stained during intracellular recording. Four neurons were injected with Lucifer yellow and two were injected with horseradish peroxidase. The shape of the rather small somata ranged from multipolar to triangular with an average soma size of 17 × 14 μm. The dendrites emerged from the poles of the somata in three or four fascicles and formed an oval-shaped dendritic field (Fig. 2*I*). Dendrites were smooth to sparsely spinous and had few branches. The axon was followed in three well-labeled neurons; it projected from the soma and arborized with dense fine processes 100–200 μm above the soma in cortical layers 3 and 4.

DISCUSSION

Neurons in the central nervous system represent a diverse collection of elements with distinct morphologies, connections, and physiological properties. One of the many properties that may differ among neurons is their ability to oscillate at particular frequencies or to serve as pacemakers. For example, segmental oscillators have been described that serve to synchronize muscular activity during locomotion or respiration (19, 20). The intrinsic properties of the inferior olive neurons have been implicated in the timing of motor sequences (1, 3), while thalamo-cortical oscillations have been associated with more general brain states such as sleep and attention (21–23). Studies in the visual cortex have identified rhythmic oscillatory potentials within cortical columns that are well correlated with single unit activity within the column and that have been proposed to serve as an associative mechanism in the temporal domain by synchronized oscillatory rhythmicity (10). This temporal association or "binding" has been demonstrated by means of cross correlation between columnal activity (10, 11). However, the neuronal source of this basic high-frequency oscillation has not been resolved. Recently, it has been proposed that the thalamus serves a linking function after conjunction, by coherent resonance, between different cortical regions (24). This view has been strengthened by the observation of 30- to 40-Hz activity during intracellular recordings from thalamic projection neurons after the activation of brain stem cholinergic inputs (25).

The findings reported here show that several classes of cortical interneurons are capable of sustained subthreshold oscillatory rhythms at frequencies similar to those found in the "activated" cortical column (10). Of these, the broad-frequency oscillators increase their frequency with membrane depolarization. This tendency may allow "coherent resonance" to occur that may facilitate phase locking of the oscillations in these neurons, depending on the level of excitatory synaptic activity in layer 4. If the broad frequency cells were to provide excitatory input to the narrow-frequency oscillators, they could, in principle, synchronize the oscillatory activity of the latter. However, the morphology and the connectivity of the broad-frequency cells are unknown.

The oscillations in these cells are generated by the alternating activation of a TTX-sensitive persistent sodium conductance and a delayed rectifier. The absence of either low-threshold or high-threshold calcium conductances enables these neurons to maintain elevated firing frequencies. Moreover, the ability of the narrow-frequency oscillators to maintain high-frequency firing from an oscillating baseline beyond the termination of the initiating stimulus can serve to sustain oscillatory activation of a cortical column.

The narrow-frequency cells have sparsely spinous to aspinous dendrites, and their axonal projection fields are consistent with their classification as cortical inhibitory interneurons (26). Only 20 narrow-frequency cells have been recorded so far primarily as a consequence of their small size. The present data suggest that these interneurons may play a role in cortical associative processing as outlined (24). The following activities would be predicted by that hypothesis. (*i*) The thalamus, by its excitatory projection to layer 4 (27), would activate the above-mentioned inhibitory interneurons that oscillate at close to 40 Hz. (*ii*) These interneurons would elicit inhibitory postsynaptic potentials (IPSPs) in other cortical neurons, including the pyramidal cells of layer 6. (*iii*) Rebound potentials triggered by these IPSPs generate rhythmic firing at 40 Hz or a harmonic frequency thereby generating the tight rhythmicity observed in the visual cortex (10). In fact, Ferster (28) has clearly demonstrated 40-Hz IPSPs in visual cortex pyramidal cells during physiological stimulation of the visual system.

This rhythmic firing of pyramidal neurons at 40 Hz would lead to synchronization across cortical columns to which the active pyramidal cells project as well as caudally (by layer 6 pyramidal cells) back to the thalamus. This descending 40-Hz rhythmic volley, by activating thalamic projection neurons and the thalamic reticularis neurons, would result in the generation of a 40-Hz excitatory postsynaptic potential–IPSP sequence in the thalamus. It must be emphasized that in awake animals reticularis neurons generate continuous trains of spikes (1). In accordance with those findings, oscillations due to rebound calcium spike mode were never seen in *in vitro* reticularis thalamic neurons in the activated (depolarized) state (29) because the low-threshold conductance is inactivated at such membrane potentials. From a functional viewpoint, rapid firing in reticularis neurons is more likely to generate the short-lasting inhibitory synaptic potentials, conducive to 40-Hz bursting in thalamic projection neurons, than it is to generate the spike bursts triggered in reticularis neurons by rebound calcium responses. That thalamic projection neurons can respond, when in the activated state, with rebound oscillations in the range of 40 Hz after short IPSP-like current injection has been recently shown *in vitro* (30). This finding demonstrates that the electrophysiological properties necessary to support 40-Hz resonation are present in thalamic cells. According to this view, the 40-Hz activation, having been initiated in the cortex and reorganized in the thalamus, would then reenter the cortex, completing a cortico-thalamo-cortical resonant loop. In principle, such conjunctive functional states could serve to bind the diverse components that constitute a given sensory input into a single cognitive experience.

Dr. Paul May kindly made the camera lucida drawing in Fig. 2. This research was supported by National Institutes of Health/National Institute of Neurological Disorders and Stroke Grants NS13742 and NS07124.

1. Steriade, M. & Llinás, R. R. (1988) *Physiol. Rev.* **68,** 649–742.
2. Steriade, M., Gloor, P., Llinás, R. R., Lopes da Silva, F. & Mesulam, M. M. (1990) *Electroencephalogr. Clin. Neurophysiol.* **76,** 481–508.
3. Llinás, R. (1984) in *Movement Disorders: Tremor,* eds. Findley, L. J. & Capiledo, R. (Macmillan, London), pp. 165–182.
4. Llinás, R. & Yarom, Y. (1986) *J. Physiol. (London)* **376,** 163–182.
5. Yarom, Y. (1989) *Exp. Brain Res. Ser.* **17,** 209–220.
6. Llinás, R. (1988) *Science* **242,** 1654–1664.
7. Alonso, A. & Llinás, R. (1989) *Nature (London)* **342,** 175–177.
8. Llinás, R. & Grace, A. A. (1989) *Soc. Neurosci. Abstr.* **15,** 660.
9. Leonard, C. & Llinás, R. (1990) in *Brain Cholinergic Systems,* eds. Steriade, M. & Biesold, D. (Oxford Univ. Press, New York), pp. 205–223.
10. Gray, C. M., Konig, P., Engel, A. K. & Singer, W. (1989) *Nature (London)* **338,** 334–337.
11. Gray, C. M., Engel, A. K., Konig, P. & Singer, W. (1990) *Eur. J. Neurosci.* **2,** 607–619.
12. Llinás, R. & Sugimori, M. (1980) *J. Physiol. (London)* **305,** 171–195.
13. Stewart, W. W. (1978) *Cell* **14,** 741–759.
14. Light, A. R. & Durkovic, R. G. (1976) *Exp. Neurol.* **53,** 847–853.
15. Snow, P. J., Rose, P. K. & Brown, A. G. (1976) *Science* **191,** 312–313.
16. Grace, A. A. & Llinás, R. (1985) *Neuroscience* **16,** 461–475.
17. Connors, B. W., Gutnick, M. J. & Prince, D. A. (1982) *J. Neurophysiol.* **48,** 1302–1320.
18. Stafstrom, C. E., Schwindt, P. D. & Crill, W. E. (1982) *Brain Res.* **236,** 221–226.
19. Wyman, R. J. (1977) *Annu. Rev. Physiol.* **39,** 417–448.
20. Pearson, K. G. (1981) *Trends Neurosci.* **4,** 128–131.
21. Steriade, M., Kitsikis, A. & Oakson, G. (1979) in *Brain Mechanisms in Memory and Learning,* ed. Brazie, M. (Raven, New York), pp. 47–52.
22. Glenn, L. L. & Steriade, M. (1982) *J. Neurosci.* **2,** 1387–1404.
23. Domich, L., Oakson, G. & Steriade, M. (1986) *J. Physiol. (London)* **379,** 429–449.
24. Llinás, R. (1990) in *Fidia Research Foundation Neuroscience Award Lectures* (Raven, New York), Vol. 4, pp. 173–192.
25. Carrodossi, R. & Pare, D. (1991) in *Induced Rhythms in the Brain,* eds. Basar, E. & Bullock, T. (Birkhaeuser, Boston), in press.
26. Jones, K. A. & Baughman, R. W. (1988) *J. Neurosci.* **8,** 3522–3534.
27. Colonnier, M. (1967) *Arch. Neurol.* **16,** 651–657.
28. Ferster, D. (1988) *J. Neurosci.* **8,** 1172–1180.
29. Llinás, R. & Geijo-Barrientos, E. (1989) in *Cellular Thalamic Mechanisms,* eds. Bentivoglio, M. & Spreafico, R. (Elsevier, Amsterdam), pp. 23–33.
30. Yarom, Y. & Llinás, R. (1990) *Soc. Neurosci. Abstr.* **16,** 955.